INITIAL MASTCAM-Z MULTISPECTRAL RESULTS FROM THE PERSEVERANCE ROVER'S EXPLORATION OF THE MARGIN UNIT IN JEZERO CRATER, MARS.

B.J Garczynski[1], J.R. Johnson[2], B. Horgan[3], A. Vaughan[4], M.S. Rice[1], J.F. Bell III[5], S. Brown[6], A. Broz[3], S. Curtis[6], M. Gabbert[1], B. Kathir[1], A. Klidaras[3], K. Lapo[1], L. Mandon[7], C. Million[6], J.I. Nuñez[2], G. Paar[8], E. Ravanis[9], M. St. Clair[6], S. Theuer[1] and the Mastcam-Z team. [1]Western Washington Univ. (garczyb@wwu.edu), [2]Johns Hopkins Univ. APL, [3]Purdue Univ., [4]Apogee Engineering LLC, [5]Arizona State Univ., [6]Million Concepts, [7]Caltech, [8]Joanneum Research, [9]Univ. of Hawai'i at Mānoa. Univ.

Introduction: The Mars 2020 Perseverance rover is currently exploring an ancient lacustrine environment at Jezero crater to characterize the regional geology, seek signs of ancient life, and cache samples for future return [1]. Since Sept. 2023, the rover has been investigating the crater's western margin ("margin unit") that exhibits strong carbonate spectral signatures from orbit previously hypothesized to be related to authigenic precipitation within the Jezero paleolake [2]. In-situ investigations have focused on constraining emplacement and alteration history of the margin unit rocks to better understand the timing and geological context within the history of Jezero crater [3]. Here we present a summary of multispectral observations collected by the Mastcam-Z instrument during the margin unit science campaign.

Mastcam-Z: The Mastcam-Z instrument is a pair of zoomable and focusable stereoscopic cameras mounted on the Perseverance rover's remote sensing mast [4]. The instrument is equipped with broadband Bayer red/green/blue (RGB) CCD-bonded filters and a set of narrowband filters that allow for visible to near-infrared (VNIR; 440-1022 nm) multispectral imaging to provide a preliminary assessment of color and mineralogical variability along the rover's traverse. The spectral range of Mastcam-Z is particularly sensitive to Fe-bearing minerals and is useful in distinguishing between primary (ferrous) and secondary (ferric) lithologies. Natural color, enhanced color, decorrelation stretch (DCS), and band parameter images are used to determine representative regions of interest (ROIs) from which spectra were extracted [5].

Multispectral observations of rocks: At outcrop scale, multispectral images acquired within the margin unit reveal massive blocks with variable pitted to granular textures that in some places exhibit evidence of internal lamination. Surface exposures of these blocks typically are fractured and form large polygons that occasionally exhibit concentric patterns. Cross-cutting filled fractures are also variably present throughout the margin unit (*Fig 1)*. In Mastcam-Z DCS composites using 1022 nm (R6), 910 nm (R3), and 800 nm (R1) filter images ("R631 DCS"), less dusty natural rock surfaces within the margin unit typically appear bright blue, typically indicating a strong NIR downturn consistent with Fe^{2+} absorptions in carbonate and/or olivine (*Fig 1*). Concentric surface features and filled fractures do not show significant color variability compared to surrounding margin unit rocks suggesting similar composition observable at Mastcam-Z scale.

Multispectral images of the two margin unit abrasion patches show these rocks are composed of a variable mixture of light- and dark-toned grains (*Fig 2)*. Grains within Amherst Point largely appear blue in the R631 DCS composite image and magenta in the spectral parameter bandmap. These grains are intermixed with surrounding matrix/grains ranging from dark green to bright orange/yellow in color as seen the in the R631 DCS image. ROI spectra of representative grains mostly exhibit strong NIR downturns with variable reflectance peaks between 677 and 754 nm consistent with a mixture of olivine and Fe-bearing carbonate. Some spectra exhibit absorptions at 528 nm consistent with Fe^{3+}. Bright orange/yellow regions (R631 DCS) are relatively spectrally neutral and suggest a composition distinct from the dominant olivine and Fe-bearing carbonate.

Compared to Amherst Point, the Bills Bay abrasion is coarser-grained, with relatively large distinct grains that appear blue in the R631 DCS image and magenta in the spectral parameter bandmap. Despite the textural differences, ROI spectra of representative grains suggest Bills Bay is also dominated by olivine and Fe-bearing carbonate although there is a notable lack of the large bright orange/yellow areas (R631 DCS) that were observed in Amherst Point.

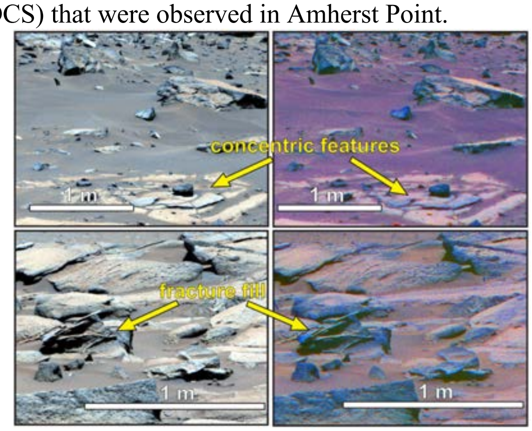

Figure 1: *Mastcam-Z right-eye enhanced color (left) and R631 DCS composite (right) images of margin unit rocks. Top – Fraser Island (sol 917 – zcam03773). Bottom – Rivoli Islands (sol 945 – zcam03804).*

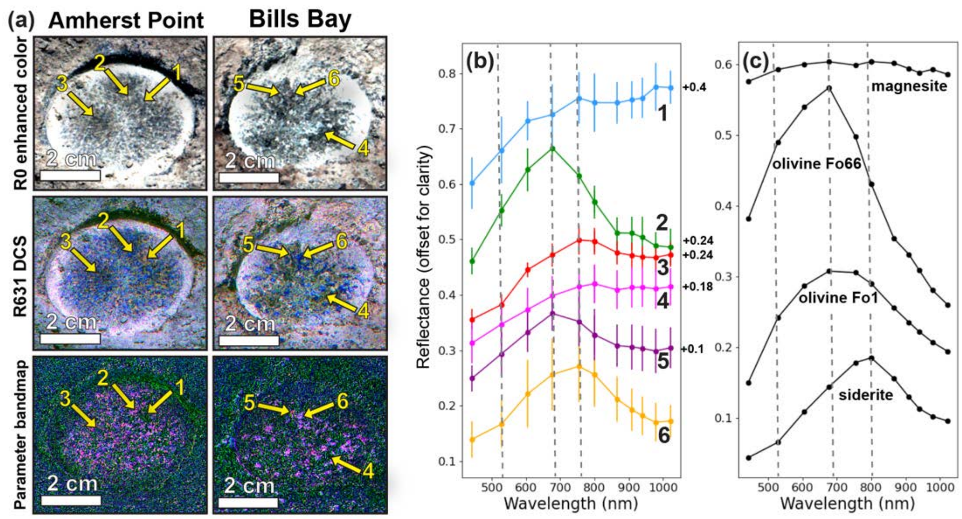

Figure2: *Mastcam-Z images of Amherst Point (zcam03772) and Bills Bay (zcam03796) abrasions, and representative ROI spectra. (a) right eye enhanced Bayer filter – top, R631 DCS composite – middle, spectral parameter bandmap (red = 634 nm/800 nm ratio, green = 910 nm band depth, blue = 800 nm/978 nm ratio) – bottom. Preliminary DCS and combined spectral parameter maps are scene dependent, and thus direct comparisons across scenes should be interpreted with caution. (b) Mastcam-Z spectra extracted from ROIs denoted by numbered arrows in (a). (c) Lab reference spectra convolved to Mastcam-Z spectral bandpasses.*

Multispectral observations of regolith: Fine and coarse regolith observed by Mastcam-Z during the margin campaign are spectrally similar, with both exhibiting reflectance peaks between 754 and 800 nm, minor absorptions near 866 nm, and a slightly positive NIR slope. These spectra are similar to those of nearby natural rock surfaces with the exception of a negative NIR slope and downturn between 978 nm and 1022 nm possibly related to differences in composition, dust cover, and/or grain size.

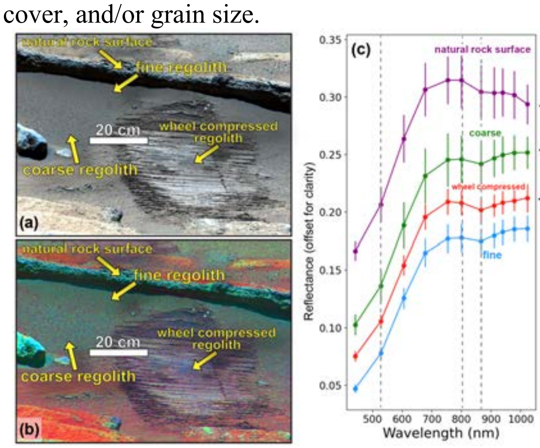

Figure 2: *Multispectral observations of sol 964 regolith target Sanberg (zcam03816)[6]. (a) Left-eye enhanced color Bayer filter image. (b) L256 DCS composite image. (c) ROI spectra of representative surfaces.*

Discussion: Mastcam-Z multispectral observations of the margin unit reveal rocks to be largely dominated by variable mixtures of olivine and Fe-bearing carbonate. Comparisons with images of abrasion patches acquired within the upper Jezero fan (to the east) reveal some similarities with notable differences [7,8]. The margin unit and upper fan both contain similar assemblages of primary mineral grains, however the margin also contains an additional component of spectrally neutral cement that may suggest the unit has a different provenance and/or diagenetic history than rocks of the upper fan. Carbonate within the margin is present as both cement and distinct grains suggesting multiple distinct origins including potential reworking of authigenic grains that may have high biosignature preservation potential. Spectrally neutral cement observed in Amherst Point could be consistent with detections of hydrated silica made by proximity science instruments [9], and the lack of similar cement detectable at Mastcam-Z scale in Bills Bay may suggest silica cementation varied with depositional facies. The presence of concentric outcrops are interpreted to be a result of spheroidal weathering or hummocky sedimentary structures [10], however spectral variability across these features is not apparent to Mastcam-Z. The presence of cross-cutting filled fractures within some margin unit rocks provide evidence that later stage fluids variably interacted with rocks to deposit vein material along fractures. Mastcam-Z spectra suggest that subsequent erosion of rocks may be contributing locally to regolith, but slight spectral differences may be related to dust and/or additional components within the regolith sourced from elsewhere.

References: [1] Farley et al. (2020) *Space Science Reviews,* 216 (8) 1-41. [2] Horgan et al. (2020) *Icarus*, 339, 113526. [3] Horgan et al., this vol. [4] Bell et al. (2021) *Space Science Reviews*, 217 (1), 1-40. [5] Rice et al. (2023) *JGR Planets.,* e2022JE007548. [6] Johnson et al., this vol. [7] Ravanis et al., this vol. [8] Nuñez et al., this vol. [9] Siljeström et al., this vol. [10] Jones et al., this vol.